Macromolecular Research
https://doi.org/10.1007/s13233-023-00190-1

Online ISSN 2092-7673
Print ISSN 1598-5032

ARTICLE

Vegetable oil-based epoxy coating materials for self-healing and anticorrosive applications

Burcu Oktay[1] · Jülide Hazal Türkcan[2] · Oğuz Kaan Özdemir[2] · Nilhan Kayaman-Apohan[1]

Received: 26 May 2023 / Revised: 18 July 2023 / Accepted: 31 July 2023

Abstract

A new bio-based epoxy curing agent from hempseed oil was prepared in this study. The chemical structure of the curing agent was confirmed by infrared spectrometry and nuclear magnetic resonance. Soybean oil-based epoxy resin was cured with a hempseed oil-based green curing agent to prepare a series of sustainable coatings under eco-friendly conditions. The reaction of epoxy resin with anhydride groups reacted without a catalyst. The prepared sustainable coatings showed excellent scratching and adhesion resistance. In addition, the coating showed self-healing properties via dynamic transesterification bonds between the epoxy and anhydride groups. The corrosion resistance of the sustainable coatings is investigated using electrochemical measurements. It revealed that the materials have strong anti-corrosion performance. Hence, these coatings can be used as a green alternative for encapsulation-based corrosion protection systems. Furthermore, the produced materials could be used as a VOC-free coating system.

Graphical abstract

A catalyst-free and environmentally friendly method was developed for the preparation of epoxy materials. The creation of bio-based epoxy hardener agents using greener techniques is a significant issue. The development of fully sustainable materials from non-edible vegetables is an attractive strategy to minimize the risk to human health and the environment.

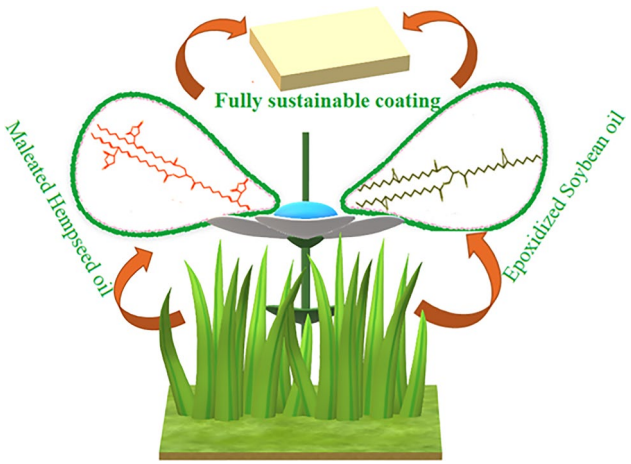

Keywords Anticorrosive coating-self-healing · Bio-based material

✉ Burcu Oktay
burcu.oktay@marmara.edu.tr

[1] Department of Chemistry, Marmara University, Goztepe, 34722 Istanbul, Turkey

[2] Department of Metallurgical and Materials Engineering, Yıldız Technical University, 34210 Istanbul, Turkey

1 Introduction

Renewable biological resources with a low environmental impact have become an attractive area for preparing bio-based materials in technological advancements [1]. Green

Published online: 14 August 2023

and natural feedstock such as cellulose, chitosan, chitin, lignin, and vegetable oils (VOs) are promising alternatives to petroleum resources [2]. In recent years, VOs have had an attractive role in the development of bio-based materials [3]. VO-based materials have been prepared as composites with the incorporation of organic and inorganic particles or polymers (polyamides, polyurethanes, polyesters, and epoxies of VOs) [4]. Because of their high availability and inexpensive cost, these materials have already been used as paint, coating, lubricant, surfactant, and food proposes [5]. Soy, castor, coconut, cotton, palm, sunflower, olive, and hemp seed oils are the most common sources of VO.

Hemp seed oil, soybean oil, and castor oil have various fatty acids containing unsaturated aliphatic alkyl chains [6]. The fatty acids of VOs have been modified from the double-double bond of unsaturated aliphatic alkyl chains [7]. Epoxidized-VOs are generally prepared by functionalization of double-double bonds using oxidizing agents at a wide range of epoxy content The epoxy modification enables the curing process with further cross-linking. Therefore, the mechanical and chemical properties of the final material can be improved [8].

Epoxidized-VOs can be cross-linked with anhydrides, aliphatic diacids, and amine cure agents to generate thermoset VO-based materials [9]. The reaction of epoxy with anhydride can undergo two pathways; with a catalyst and without a catalyst. The use of catalysts is generally preferred to prevent prolonged curing times for achieving higher cross-linking efficiency. It is known that high-performance material property is related to high cross-linking density. However, vegetable-based systems exhibit low cross-linking density. To overcome this situation, epoxidized-VOs are blended with petrochemical-based resins [10–12].

The mobility of cured epoxy chains is limited due to a stable cross-linked network. The stable network causes restrict repairability of material. Therefore, the service life of the coatings is reduced and the replacement time of the coating is shortened [13]. Altuna et al. prepared a new thermoset material composed of epoxidized soybean oil and citric acid. The resulting material exhibited self-healable properties at 160 °C [14]. In another study, Liu et al. synthesized rosin-based thermoset hydrogels having dynamic covalent bonds [15]. Some dynamic covalent bonds such as imine, hydroxyl-ester, Diels–Alder, and disulfide provide the repairability of coating. Dynamic hydroxyl-ester bonds are the best-approved linkage for epoxy-anhydride and epoxy-acid systems. Internal epoxy groups of epoxidized-VO are less reactive compared to terminal epoxy groups. Therefore, the epoxidized-VO shows low polymerization efficiency with amine cure agents [10]. In addition, the by-product can be formed during the reaction of epoxy and amine [11]. Catalyst-free grafting of dynamic transferrable mono-esterified cyclic anhydrides into epoxy networks provides re-processability and rapid stress relaxation. Liu et al. studied network re-arrangement of the bisphenol A epoxy DER 331 with cyclic anhydride [16]. Yang et al. prepared innovative self-healable materials from epoxidized soybean oil and rosin derivative-fumaropimaric acid using zinc acetylacetonate as a transesterification catalyst [17].

In this study, we synthesized cyclic anhydride modified-hempseed oil (HOMA) by the reaction of hempseed oil (HO) and maleic anhydride. The vegetable-based polyester coating materials were prepared with HOMA and epoxidized-SO (ESO) in one-step method without using any solvent or catalyst. The structural characterization of HOMA was investigated by infrared spectroscopy and nuclear magnetic resonance spectroscopy (NMR). The thermal properties of the cured coating and films were monitored by gravimetric analysis and differential scanning calorimetry (DSC). The mechanical properties of the films were characterized by tensile tests. The coating properties of the materials such as contact angle, hardness, scratch resistance, flexibility, and adhesion were also tested. In addition, the self-healing and anti-corrosion properties of the cured films were investigated.

2 Experimental section

2.1 Materials

Epoxidized soybean oil and maleic anhydride (99%) was supplied by Sigma-Aldrich. Hempseed oil (HO) was provided by a local market.

2.2 Synthesis of maleinized hempseed oil (HOMA)

Maleinization of HO was adapted from the literature procedures [18–20]. A three-neck round flask was equipped with a reflux condenser and a nitrogen gas atmosphere. 100 g of HO was charged into the flask and the temperature was gradually raised from 180 to 220 °C for 2 h. 10 g of maleic anhydride was added into the flask in pieces for 2 h. The mixture was further stirred for 1 h at 220 °C. Finally, the flask was cooled down to room temperature. To remove unreacted maleic anhydride, the mixture was diluted with cold diethyl ether and washed with water three times. Diethyl ether was evaporated via a rotary evaporator and dried under a vacuum. The reaction pathway is shown in Scheme 1.

The maleinization degree was found by measuring the acid number with the following equation:

$$\text{Acid number} = (56.01 \times V \times c)/m,$$

where V and c are the volume and concentration of the KOH standard solution and m is the mass of HOMA.

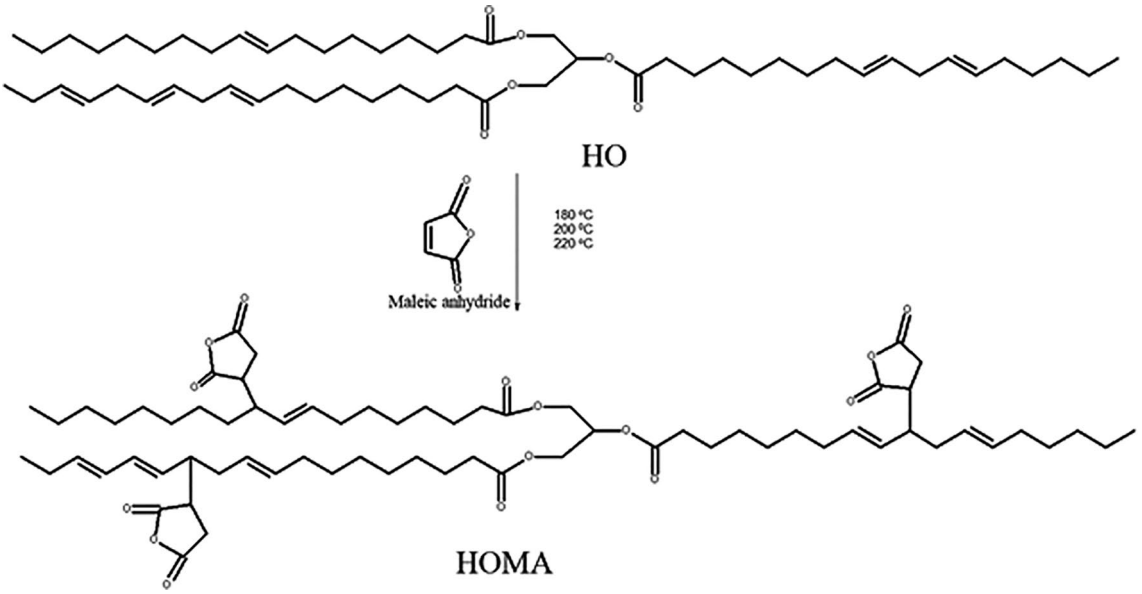

Scheme 1. Maleinization of hempseed oil

2.3 Preparation of films

The compositions of fully bio-based were prepared with anhydride/epoxy ratios 1, 1.2, 1.5, and 2. The curing formulations at different ratios of ESO and HOMA were prepared in a beaker without adding any catalyst. After homogenization, the beakers were placed in an oven to remove air bubbles. Each formulation was placed into Teflon® molds (10 mm × 50 mm × 1 mm). In addition, the temperature gradually increased from 60 °C to the cure temperature of each sample in the air. The codes of the prepared films were associated with the anhydride/epoxy ratios as HOMA-ESO-1, HOMA-ESO-1.2, HOMA-ESO-1.5, and HOMA-ESO-2. The reaction pathway is shown in Scheme 2.

2.4 Characterization

The chemical structures were identified by FTIR (Perkin–Elmer Spectrum 100 ATR-FTIR Spectrophotometer) and 1H-NMR (Mercury-VX 400 MHz Spectrometer)

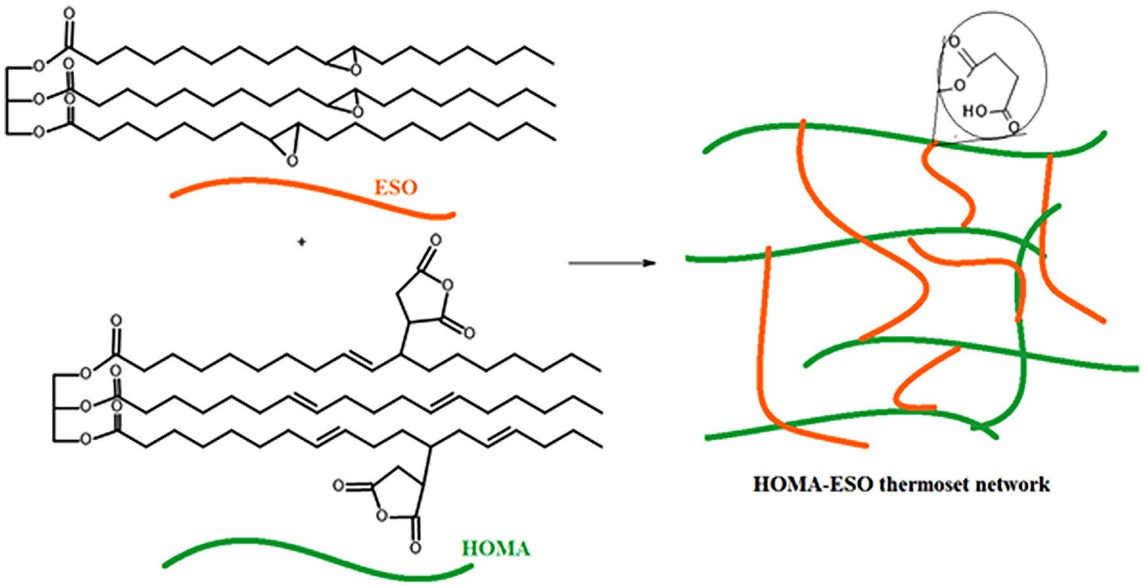

Scheme 2. The reaction pathway of HOMA and ESO

spectroscopies. The coating properties were measured by the corresponding standard test methods as indicated. These include crosscut adhesion (DIN 53151), pendulum hardness (DIN 53157), and Erichsen test (DIN53156). Thermogravimetric analysis (TGA) of the films was performed by Perkin Elmer STA6000. SEM images of the films were analyzed on Philips XL30 ESEM-FEG/EDAX. DSC measurements were performed using Pyris Diamond DSC. The mechanical properties of the films were determined using Zwick Z010 Universal Tensile Tester with a crosshead speed of 10 mm/min. The contact angle measurement of the cured coatings was measured with Kruss Easy Drop DSA-2. The surface energy of the coatings was calculated. Three solutions used were water and ethylene glycol as polar solvents and iodomethane as a dispersed solvent. Corrosion tests were conducted according to our previous work [21].

3 Results and discussions

3.1 Structural analysis

HOMA was prepared by reacting HO and maleic anhydride. The product was characterized via FTIR and ^{1}H-NMR spectroscopy techniques. Figure 1 shows the FTIR spectrum of HO and HOMA. The characteristic peaks at 3005 and 722 cm^{-1} are attributed to the double bond of fatty oil. The peaks at 2920, 2852, and 1460 cm^{-1} correspond to CH– stretching in the HO. The band at 1742 cm^{-1} is attributed to C=O stretching. After the grafting of maleic anhydride, the characteristic anhydride peaks at 1800, 1780, and 921 cm^{-1} were observed. The carbonyl peak of HO was observed at 1736 cm^{-1}. The peaks at 1224, 1155 and 1070 cm^{-1} are due to the C-O stretching of maleic anhydride [20]. The peak at 1162 cm^{-1} is attributed to the bending of the C–H group of the anhydride ring [22].

The NMR spectra of HO and HOMA are given in Figs. 2 and 3. The peaks at 4.0–4.2 ppm are the methylene protons of the glycerol unit in HO (Fig. 2). The methylene protons of double bonds were observed at 5.1–5.3 ppm. The peaks at 2.0–2.3 ppm were attributed to methylene protons on HO. In the NMR spectrum of HOMA (Fig. 3), the protons of the two methylenes in the maleic anhydride ring appeared at 2.5–3.0 ppm. Furthermore, the methylene protons between two double bonds completely disappeared [4]. These results show that maleic anhydride groups grafted on HO chains.

3.2 Compositions of films

The fully bio-based films were prepared by epoxy-anhydride polymerization with a non-catalyzed process. Hydroxyl groups of ESO initiate the un-catalyzed reaction through an attack on the anhydride group of HOMA and produce the polyester chains with an active carboxyl end group. The free carboxyl groups react with epoxy groups and then epoxy groups react with another epoxy group [23]. Generally, most of the epoxy-anhydride cure systems based on epoxidized vegetable oil are often blended with petrochemical-based epoxy systems due to inadequate cross-linking density. Commercial epoxy resin is generally used for 60% of the total amount [10]. Therefore, bio-based content is reduced in the final product. For this study, the fully bio-based films were prepared from vegetable-based oil derivatives; ESO, and HOMA with an un-catalyzed process.

The films were prepared with anhydride/epoxy ratios 1, 1.2, 1.5, and 2. On the other hand, the fully cured film could

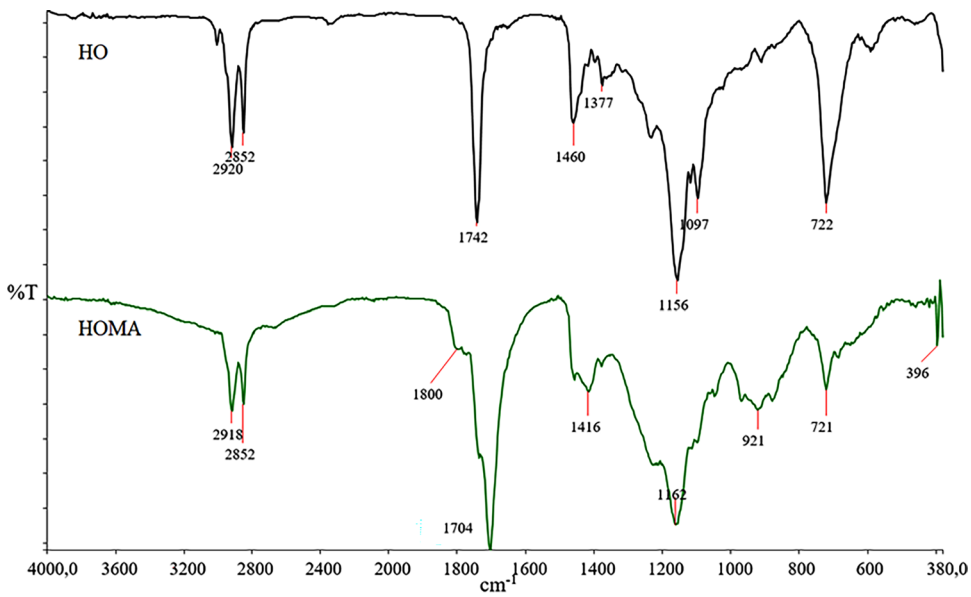

Fig. 1 FTIR spectra of HO and HOMA

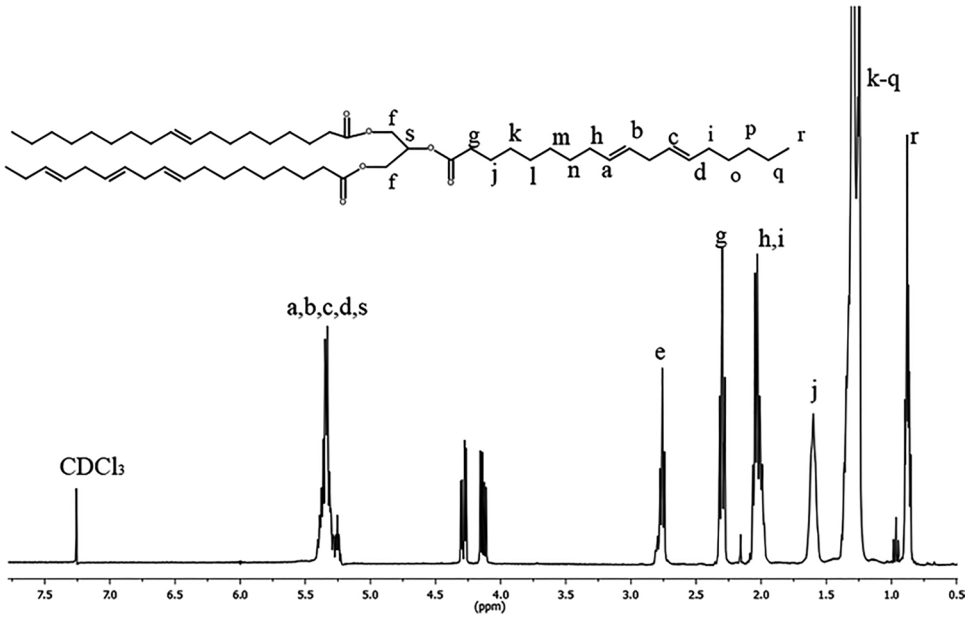

Fig. 2 [1]H-NMR spectra of HO

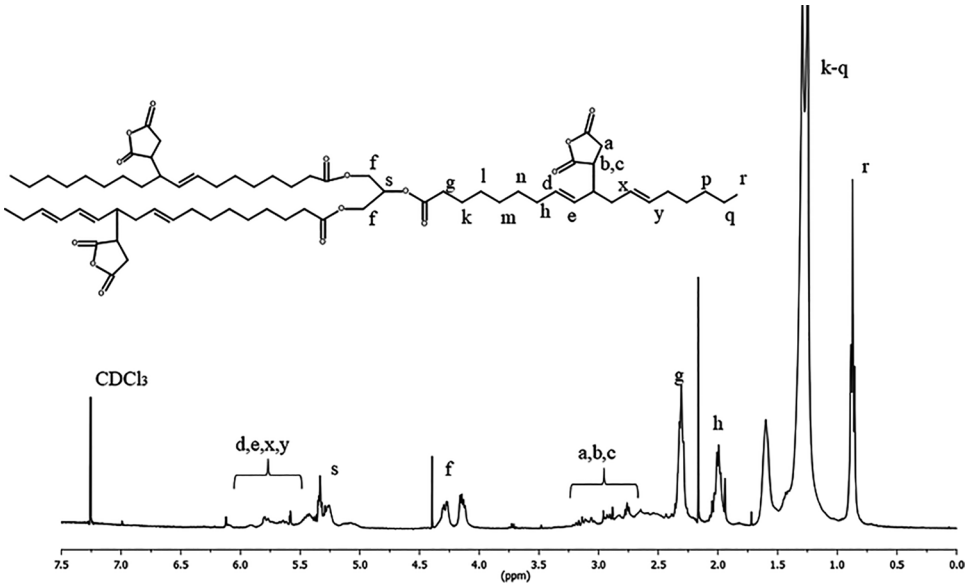

Fig. 3 [1]H-NMR spectra of HOMA

not be prepared with a molar ratio of less than 1. Homopolymerization of epoxy occurs at insufficient anhydride content at high temperatures, and epoxy resin disintegrates [24, 25].

The exothermic curing profiles of the fully bio-based films were investigated (in Fig. S1). All samples exhibited a single exothermic peak in the range of 97 and 135 °C. The peaks shifted to lower and higher cure temperatures with the ESO content.

On the other hand, the fully bio-based films showed high gel content of 87–93% (Table 1). The high gel content indicates that the epoxy-anhydride system is well cured. With the increase in the ESO ratio, the gel content declined from 93 to 87. This is probably due to the steric hindrance effect of longer carbon chains of ESO [26].

Table 1 Contact angle and surface free energy of the coatings

Samples	Water (°)	Diiodomethane (°)	Surface energy (mN/m)
HOMA-ESO-1 (HOMA2)	86	50	33.4
HOMA-ESO-1.2 (HOMA4)	85	37	33.0
HOMA-ESO-1.5 (HOMA5)	83	40	34.8
HOMA-ESO-2 (HOMA1)	82	33	39.4

Figure 4 shows the FTIR spectra of all films. For HOMA-ESO-1 and HOMA-ESO-1.2, the characteristic anhydride peaks at 1853 and 1780 cm^{-1} disappeared. However, a new

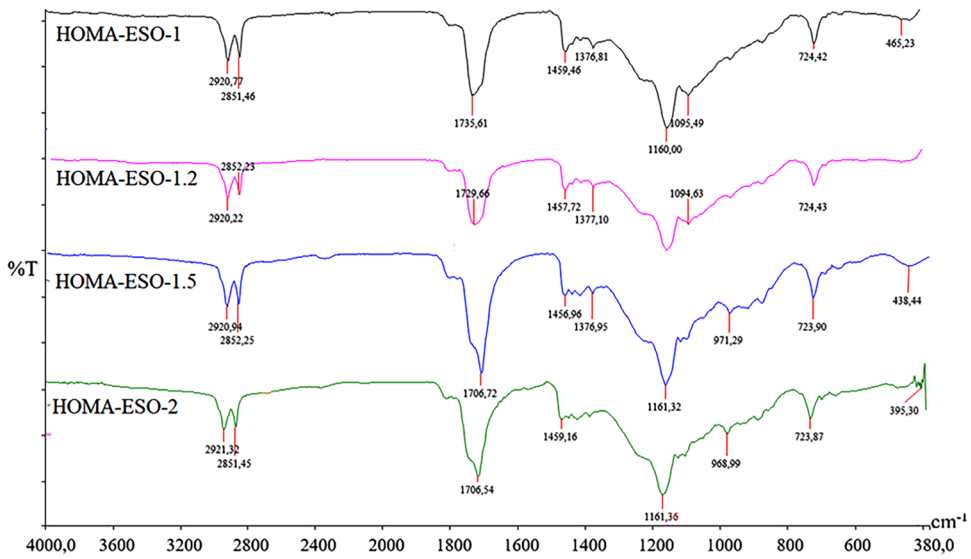

Fig. 4 FTIR spectra of cured film samples

carbonyl ester peak occurred at 1735 cm^{-1}. The formation of the ester peak and the disappearance of anhydride peaks indicate that the anhydride and epoxy groups are fully connected. For HOMA-ESO-1.5 and HOMA-ESO-2, the anhydride carbonyl peaks disappeared. Furthermore, the ester carbonyl was observed at 1735 cm^{-1}. The anhydride/epoxy molar ratio increased to 1.5 and 2, and pendant carboxylate groups were observed at about 1710 cm^{-1}. Excess anhydride groups further cannot react with epoxy groups in the epoxy-anhydride system. Therefore, ester carbonyl is dominant in the molar ratio 1 and 1.2. In contrast, carboxylate groups are more dominant in the molar ratios 1.5 and 2.10.

3.3 Surface properties of the coating

The surface properties of the coatings were investigated by contact angle and surface free energy measurements. The results are shown in Table 1. In addition, the water contact angle images are presented in Fig. S2. The wettability of the cured materials is affected by the content of ESO. As can be seen, the contact angle decreased with an increasing amount of ESO. The anhydride/epoxy mixing ratio is larger than 1, increasing the number of polar groups on the surface of the films. As known, polar groups decrease the contact angle of a coating [27, 28]. The surface polar groups led to a decrease in hydrophobic character. Therefore, the surface energy values of the coating increase. Generally, silicone, fluorine oligomers, and surface roughness cause a decrease in oleophobic character [29].

3.4 Physical properties of the coating

The physical properties of cured coatings are presented in Table 2. The scratch resistance of the cured coatings was evaluated by the pencil hardness test. The scratch resistance of the coatings is 5H except for HOMA-ESO-1.

The results of the crosscut adhesion test showed that the formulations well adhered to metal surfaces. HOMA-ESO-1 showed a high pendulum hardness (42 s^{-1}) value in comparison to other samples. As can be seen, the concentration of ionic groups on the surface affects hardness [30].

Furthermore, a tea and coffee test was performed on the coating surface. The tea and coffee were first applied to the coating surface in small pools and in contact with the coating for 24 h at room temperature. Tea and coffee pools do not affect the coatings.

Erichsen cupping test values of the cured coatings are presented in Table 2. The cupping test is a measure of flexibility under pressure. The Erichsen cupping shows the elongation in mm. There is a relation between

Table 2 The physical properties of the cured coatings

Samples	Gel content (%)	Pencil hardness	Cross-cut	Pendulum hardness (s^{-1})	Tea and coffee effect	Erichsen cupping test (mm)
HOMA-ESO-1	87	2H	0	42	No effect	8.2
HOMA-ESO-1.2	91.3	5H	0	32	No effect	8.8
HOMA-ESO-1.5	91.1	5H	0	30	No effect	> 8.8
HOMA-ESO-2	93	5H	0	28	No effect	8.0

flexibility and the cupping test [31, 32]. As can be seen from Erichsen cupping results, the cured coatings showed high flexibility and were linearly related to pendulum hardness results. HOMA-ESO-1.5 is the most flexible (> 8.8 mm) and the other samples are also flexible. The Erichsen cupping test digital images of the cured coatings are shown in Fig. S3.

3.5 Thermal analysis of coatings

The thermal property of the fully bio-based films was investigated via thermal gravimetric analysis (TGA). The TGA curves are given in Fig. S4. All samples showed a single-step degradation curve between 300 and 480 °C, which is related to the degradation of the main backbone.

Tg values of the cured films are 17, 14, 6, and 5 °C for the HOMA-ESO-1, HOMA-ESO-1.2, HOMA-ESO-1.5, and HOMA-ESO-2 samples, respectively. T_g of the cured films decreased as the molar ratio of the anhydride group/epoxy group was further increased to > 1 since there are not enough epoxy groups in the system to fully consume the carboxyl groups. The amount of free carboxyl groups increases with decreasing ESO content. As a result of lower cross-linking density, the polymer network exhibits a lower T_g value [16]. T_g values of the studying systems based on epoxidized vegetable oil were reported ranging from − 5 to 65 °C [33].

3.6 Mechanical properties of coatings

The detailed data on tensile properties are presented in Table 3. Vegetable oil thermoset materials generally show low modulus values. For example, Webster et al. prepared soybean oil-based thermosets with the 1.38 and 0.22 MPa modulus [34]. For this study, the cross-linked films exhibited low modulus and high elongation at break as expected. Young's modulus of the cured films had close to each other. However, the elongation at the break of the film tends to increase. Generally, as the structure of the film softened, the elongation increased [35].

3.7 Self-healing performance of the coating

The self-healing performance of films was investigated. The cured films are entirely cut into two parts using a blazer blade. Then the two parts of the film were re-adhered by subsequently pressed at 140 °C for 4 h. Flexible films turn out to be rigid materials. Young's modulus of the self-heal films drastically increased. However, elongation at break decreased. This change is most probably due to forming of strong ester bonds. Carboxyl groups in the cross-linked network structure should have some catalytic impact. Therefore, a transesterification reaction occurred [16, 36].

The self-healing performance of the cured films was followed by SEM analysis. The fractured surfaces of the film samples can be seen in Figs. 5 and 6. As can be seen from Fig. 5, two parts completely adhered to each other at the interface. The new ester bonds produced during the curing process of ESO and HOMA in the resulting cross-linked network. The cured film exhibited self-healable properties due to the dynamic transesterification reaction of the ester bonds in the cross-linked network and hydroxyl groups of ESO [37].

3.8 Morphological analysis

The miscibility of ESO and HOMA components with each other in all ratios was confirmed by SEM images. SEM images from the surfaces of the films are shown in Fig. S5. Hempseed and soybean oils are homogeneously dispersed within each other without phase separation. This may be related to the plasticizer effects of oils.

3.9 Corrosion performance

The corrosion resistance of the fully bio-based films was evaluated by the potentiodynamic polarization method using the extrapolation method. Figure 7 and Table 4 show Tafel plots of the film in NaCl solution and their results, respectively. The results revealed that E_{corr} values shifted towards the higher value (more positive) and I_{corr} values are lower with the increase in ESO content. Lower I_{corr} and higher E_{corr} values are common in promising anticorrosive coatings,

Table 3 Mechanical properties of the cured films before and after self-healing

Samples	Before self-healing			After self-healing		
	Modulus (MPa)	Tensile strength (MPa)	Elongation at break (%)	Modulus (MPa)	Tensile strength (MPa)	Elongation at break (%)
HOMA-ESO-1	0.67	0.25	49.17	2.22	0.95	26.42
HOMA-ESO-1.2	0.60	0.37	55.57	2.50	1.00	24.22
HOMA-ESO-1.5	0.95	0.79	95.32	7.41	1.11	19.00
HOMA-ESO-2	0.96	0.22	97.03	27.70	0.94	14.37

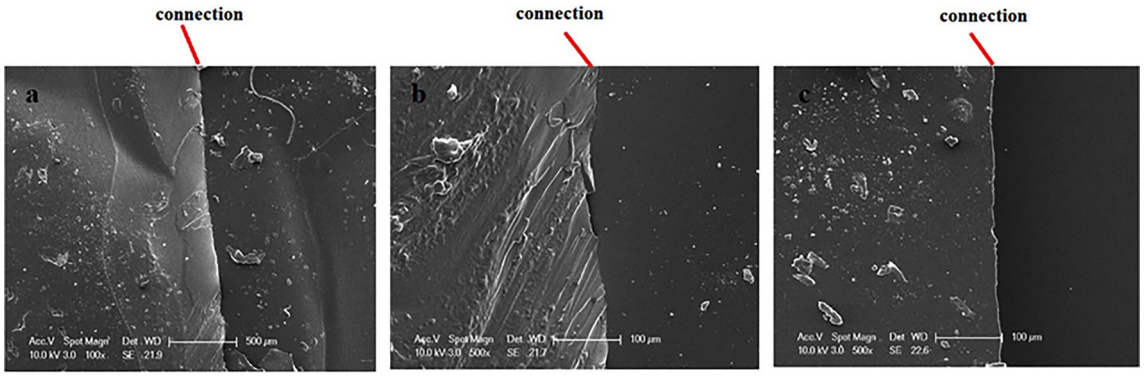

Fig. 5 SEM images of **a** HOMA-ESO-1, **b** HOMA-ESO-1.2 and **c** HOMA-ESO-2

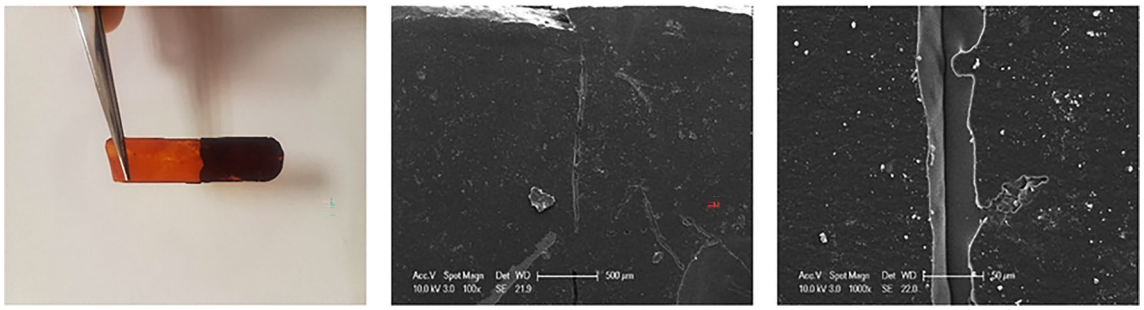

Fig. 6 Digital and SEM images of HOMA-ESO-1.5

Fig. 7 LSV curves of the samples

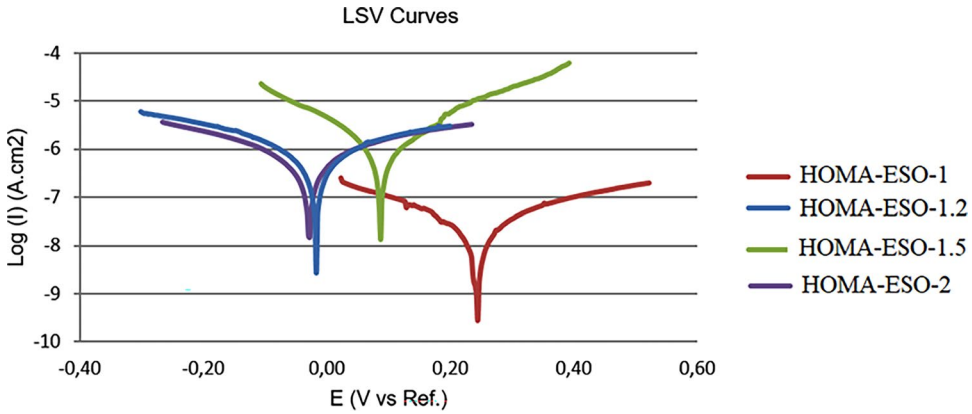

Table 4 Corrosion potential (E_{corr}) and corrosion current (I_{corr}) values of the samples

Samples	E_{corr} (mV)	I_{corr} (μA cm^{2-})
HOMA-ESO-1	0.240	2.75 10^{-4}
HOMA-ESO-1.2	0.02	2.69 10^{-4}
HOMA-ESO-1.5	0.09	1.37 10^{-2}
HOMA-ESO-2	0.03	1.66 10^{-2}

resulting in relatively low corrosion rates [38]. All the prepared full bio-based films exhibited higher corrosion resistance. The films show barrier properties and the barrier layer is the transition of water and corrosive ions (such as Cl−) dissolved [39–41].

The coated panels were immersed in 3.5% NaCl solution for the salt-spray test for 14 days. The digital images of the coating surfaces are shown in Supplement Fig. S6 after and before. The coating showed good corrosion resistance. The hydrophobic coating showed water-repelling properties on the surface. The hydrophobicity of the coating surfaces also

provides a barrier in the metal interface and inhibits the diffusion of corrosive groups through the surface of the coating [42]. The coatings continued self-healing properties after immersion in the salt solution. The immersed panels were again heated at 140 °C for 2 h in an oven.

4 Conclusion

HOMA-ESO-based thermosets were created through a green pathway. The bio-based coatings and films were cured with different stoichiometric ratios of epoxy-anhydride. The materials exhibited high elongation at break and well flexibility. The pendulum hardness values of the coatings are between 28 and 42 s^{-1}. The coating provided excellent corrosion protection. Furthermore, the bio-based materials showed self-healing properties via dynamic transesterification reaction. The created coating materials reveal that it has possible uses as a low-cost and VOC-free coatings system when compared to previously described methods.

Supplementary Information The online version contains supplementary material available at https://doi.org/10.1007/s13233-023-00190-1.

Availability of data and materials Supporting information available.

Declarations

Conflict of interest The authors have no conflicts of interest to disclose.

References

1. X. Piao, M. Xie, X. Duan et al., Novel high-performance bamboo modification through nature rosin-based benzoxazine. Constr. Build. Mater. **319**, 126123 (2022)
2. N.A. Al-Tayyar, A.M. Youssef, R.R. Al-Hindi, Edible coatings and antimicrobial nanoemulsions for enhancing shelf life and reducing foodborne pathogens of fruits and vegetables: a review. Sustain. Mater. Technol. **26**, e00215 (2020)
3. U. Biermann, U. Bornscheuer, M.A.R. Meier et al., Oils and fats as renewable raw materials in chemistry. Angew. Chemie. Int. Ed. **50**, 3854–3871 (2011)
4. R. Li, P. Zhang, T. Liu et al., Use of hempseed-oil-derived polyacid and rosin-derived anhydride acid as cocuring agents for epoxy materials. ACS Sustain. Chem. Eng. **6**, 4016–4025 (2018)
5. L. Montero De Espinosa, M.A.R. Meier, Plant oils: The perfect renewable resource for polymer science. Eur. Polym. J. **47**, 837–852 (2011)
6. M. Alam, N.M. Alandis, Development of ambient cured polyesteramide coatings from linseed oil: a sustainable resource. J. Polym. Environ. **19**(2), 391–397 (2011)
7. M. Moreno, M. Goikoetxea, M.J. Barandiaran, Biobased-waterborne homopolymers from oleic acid derivatives. J. Polym. Sci. Part A Polym. Chem. **50**, 4628–4637 (2012)
8. V. Sharma, P.P. Kundu, Addition polymers from natural oils—a review. Prog. Polym. Sci. **31**, 983–1008 (2006). https://doi.org/10.1016/J.PROGPOLYMSCI.2006.09.003
9. C. Di Mauro, S. Malburet, A. Genua et al., Sustainable series of new epoxidized vegetable oil-based thermosets with chemical recycling properties. Biomacromol **21**, 3923–3935 (2020)
10. A. Paramarta, D.C. Webster, Bio-based high performance epoxy-anhydride thermosets for structural composites: the effect of composition variables. React. Funct. Polym. **105**, 140–149 (2016)
11. A. Gandini, T.M. Lacerda, A.J.F. Carvalho, A straightforward double coupling of furan moieties onto epoxidized triglycerides: synthesis of monomers based on two renewable resources. Green Chem. **15**, 1514–1519 (2013)
12. J. Van Haveren, E.A. Oostveen, F. Micciche, B.A.J. Noordover, C.E. Koning, R.A.T.M. Van Benthem, J.G.J. Weijnen, Resins and additives for powder coatings and alkyd paints, based on renewable resources. J. Coat. Technol. Res. **4**(2), 177–186 (2007)
13. S. Zhang, T. Liu, C. Hao et al., Hempseed oil-based covalent adaptable epoxy-amine network and its potential use for room-temperature curable coatings. ACS Sustain. Chem. Eng. **8**, 14964–14974 (2020)
14. F.I. Altuna, V. Pettarin, R.J.J. Williams, Self-healable polymer networks based on the cross-linking of epoxidised soybean oil by an aqueous citric acid solution. Green Chem. **15**, 3360–3366 (2013)
15. M.M. Perera, N. Ayres, Dynamic covalent bonds in self-healing, shape memory, and controllable stiffness hydrogels. Polym. Chem. **11**, 1410–1423 (2020)
16. Y. Liu, S. Ma, Q. Li et al., Dynamic transfer auto-catalysis of epoxy vitrimers enabled by the carboxylic acid/epoxy ratio based on facilely synthesized trifunctional monoesterified cyclic anhydrides. Eur. Polym. J. **135**, 109881 (2020)
17. X. Yang, L. Guo, X. Xu et al., A fully bio-based epoxy vitrimer: self-healing, triple-shape memory and reprocessing triggered by dynamic covalent bond exchange. Mater. Des. **186**, 108248 (2020)
18. A. Carbonell-Verdu, D. Garcia-Garcia, F. Dominici et al., PLA films with improved flexibility properties by using maleinized cottonseed oil. Eur. Polym. J. **91**, 248–259 (2017)
19. A. Lerma-Canto, J. Gomez-Caturla, M. Herrero-Herrero et al., Development of polylactic acid thermoplastic starch formulations using maleinized hemp oil as biobased plasticizer. Polymer **13**, 1392 (2021)
20. T. Eren, S.H. Küsefoğlu, R. Wool, Polymerization of maleic anhydride–modified plant oils with polyols. J Appl Polym Sci **90**, 197–202 (2003)
21. S. Akhan, B. Oktay, O.K. Özdemir, S. Madakbaş, N.K. Apohan, Polyurethane graphene nanocomposites with self-healing properties by azide-alkyne click reaction. Mater. Chem. Phys. **254**, 123315 (2020)
22. B.-G. Gordana, A. Grozdanov, Poly(3-hydroxybutyrate-co-3-hydroxyvalerate)-based biocomposites reinforced with kenaf fibers. J. Appl. Polym. Sci. **104**, 3192–3200 (2007)
23. J.J. Licari, D.W. Swanson, Chemistry, formulation, and properties of adhesives. Adhes. Technol. Electron. Appl. **28**, 95–168 (2005)
24. M.C. Di, A. Genua, A. Mija, Building thermally and chemically reversible covalent bonds in vegetable oil based epoxy thermosets. Influence of epoxy–hardener ratio in promoting recyclability. Mater. Adv. **1**, 1788–1798 (2020)
25. W. Zhao, L. An, S. Wang, Recyclable high-performance epoxy-anhydride resins with DMP-30 as the catalyst of transesterification reactions. Polymers (Basel) **13**, 1–18 (2021)
26. X. Yang, C. Wang, S. Li et al., Study on the synthesis of bio-based epoxy curing agent derived from myrcene and castor oil and the properties of the cured products. RSC Adv. **7**, 238–247 (2016)
27. J.F. Wu, S. Fernando, K. Jagodzinski et al., Effect of hyperbranched acrylates on UV-curable soy-based biorenewable coatings. Polym. Int. **60**, 571–577 (2011)

28. R. Liu, J. Zhu, J. Luo, X. Liu, Synthesis and application of novel UV-curable hyperbranched methacrylates from renewable natural tannic acid. Prog. Org. Coat. **77**, 30–37 (2014)
29. A. Bendahou, A. Hajlane, A. Dufresne, S. Boufi, H. Kaddami, Esterification and amidation for grafting long aliphatic chains on to cellulose nanocrystals: a comparative study. Res. Chem. Intermed. **41**, 4293–4310 (2015)
30. H. Bakhshi, H. Yeganeh, S. Mehdipour-Ataei, Synthesis and evaluation of antibacterial polyurethane coatings made from soybean oil functionalized with dimethylphenylammonium iodide and hydroxyl groups. J. Biomed. Mater. Res. A **101**, 1599–1611 (2013)
31. S. Karataş, Z. Hoşgör, Y. Menceloğlu et al., Synthesis and characterization of flame retarding UV-curable organic–inorganic hybrid coatings. J. Appl. Polym. Sci. **102**, 1906–1914 (2006)
32. R. Schwalm, L. Häußling, W. Reich et al., Tuning the mechanical properties of UV coatings towards hard and flexible systems. Prog. Org. Coat. **32**, 191–196 (1997)
33. A.E. Gerbase, C.L. Petzhold, A.P.O. Costa, Dynamic mechanical and thermal behavior of epoxy resins based on soybean oil. J. Am. Oil. Chem. Soc. **79**, 797–802 (2002)
34. X. Pan, D.C. Webster, Impact of structure and functionality of core polyol in highly functional biobased epoxy resins. Macromol. Rapid Commun. **32**(17), 1324–1330 (2011)
35. K. Ekthamasut, A. Akesowan, Effect of vegetable oils on physical characteristics of edible Konjac films. AU J. Technol. **5**(2), 2022 (2001)
36. M. Delahaye, J.M. Winne, F.E. Du Prez, Internal catalysis in covalent adaptable networks: phthalate monoester transesterification as a versatile dynamic cross-linking chemistry. J. Am. Chem. Soc. **141**, 15277–15287 (2019)
37. M. Fei, T. Liu, B. Zhao et al., From glassy plastic to ductile elastomer: vegetable oil-based UV-curable vitrimers and their potential use in 3D printing. ACS Appl. Polym. Mater. **3**, 2470–2479 (2021)
38. O.U. Rahman, S.I. Bhat, H. Yu, S. Ahmad, Hyperbranched soya alkyd nanocomposite: a sustainable feedstock-based anticorrosive nanocomposite coatings. ACS Sustain. Chem. Eng. **5**, 9725–9734 (2017)
39. X. Zhang, J. Liang, B. Liu, Z. Peng, Preparation of superhydrophobic zinc coating for corrosion protection. Colloids Surf. A Physicochem. Eng. Asp. **454**, 113–118 (2014)
40. T. Jin, F.M. Kong, R.Q. Bai, R.L. Zhang, Anti-corrosion mechanism of epoxy-resin and different content Fe_2O_3 coatings on magnesium alloy. Front. Mater. Sci. **10**(4), 367–374 (2016)
41. J. Ou, W. Hu, M. Xue et al., Superhydrophobic surfaces on light alloy substrates fabricated by a versatile process and their corrosion protection. ACS Appl. Mater. Interfaces **5**, 3101–3107 (2013)
42. Advances in smart coatings and thin films for future industrial and biomedical engineering applications—1st edition. https://www.elsevier.com/books/advances-in-smart-coatings-and-thin-films-for-future-industrial-and-biomedical-engineering-applications/makhlouf/978-0-12-849870-5. Accessed 26 Jan 2022